

Supplementary Figures

for

“Past matrix stiffness primes epithelial cells and regulates their future collective migration through a mechanical memory”

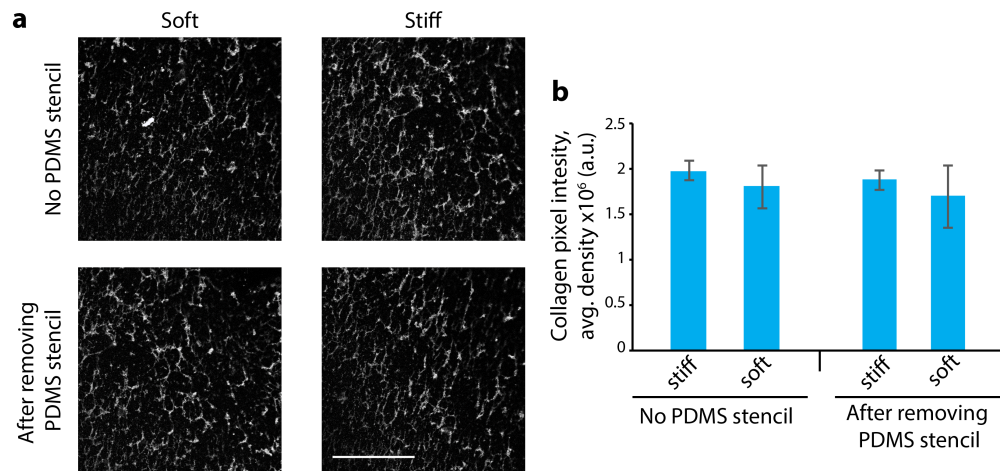


Figure S1: Collagen I coating on soft and stiff PA gels. Rat-tail collagen type I was labelled using Sulfo-Cyanine5 NHS ester, as described previously*. **(a)** Soft (0.5 kPa) and stiff (50 kPa) PA gels coated with 0.05 mg/ml of this labeled collagen I were imaged. Scale bar = 50 μm . **(b)** The integrated density of pixel intensity measured from these collagen images shows insignificant difference in soft and stiff gels. These measurements were repeated after removing the PDMS stencil, which shows robust collagen coating with or without PDMS interaction.

* Doyle AD, Carvajal N, Jin A, Matsumoto K, & Yamada KM (2015) Local 3D matrix microenvironment regulates cell migration through spatiotemporal dynamics of contractility-dependent adhesions. *Nature communications* 6:8720.

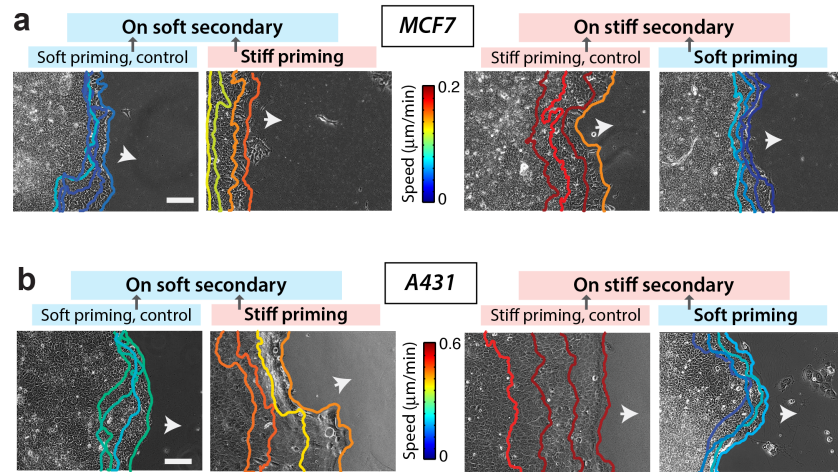


Figure S2: Leading-edge tracks of representative monolayers of MCF7 and A431 cells. Plots describing the leading-edge tracks of representative monolayers of (a) MCF7 and (b) A431 cells recorded for 12 hours after entering the secondary ECM; tracks color-coded based on the leading-edge migration speed. In each case, four representative leading-edge tracks at 3 h interval are plotted on soft or stiff secondary ECMs, which were previously primed on stiff or soft primary ECMs. Arrows indicate the general direction of migration. Scale bar = 100 μm.

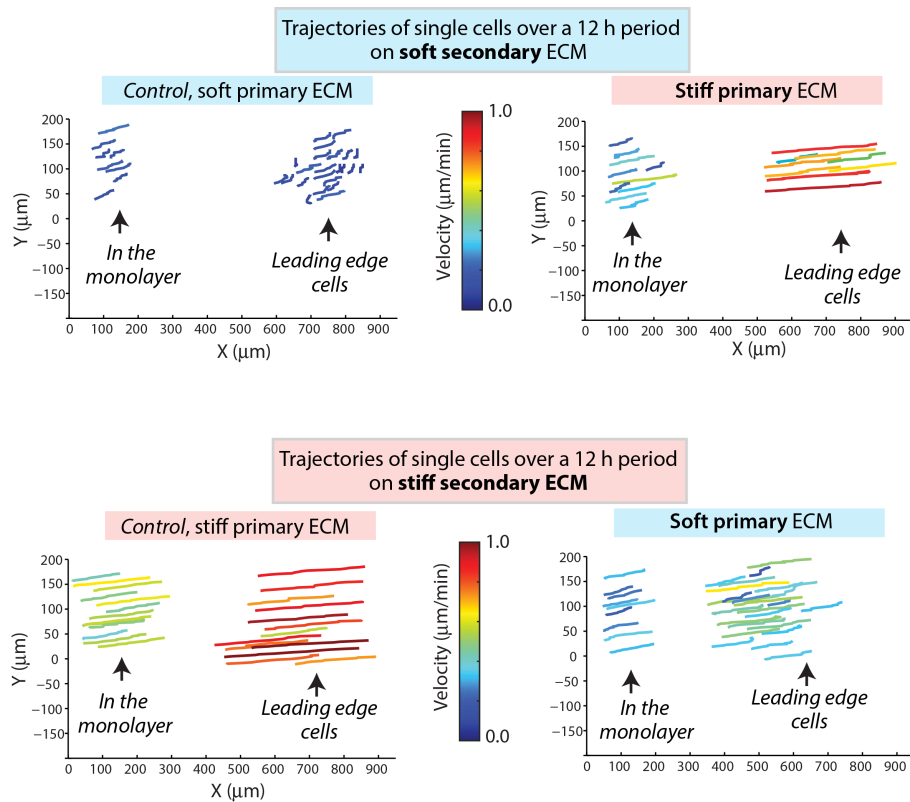


Figure S3: Single cell trajectories within the migrating monolayer. Trajectories of single cells located at the leading edge and inside (at least 200 μm behind the leading edge) the monolayer of cells migrating on soft (top) or stiff (bottom) secondary ECM, after priming on soft or stiff primary ECMs. Tracks were color coded according to migration speed for each cell.

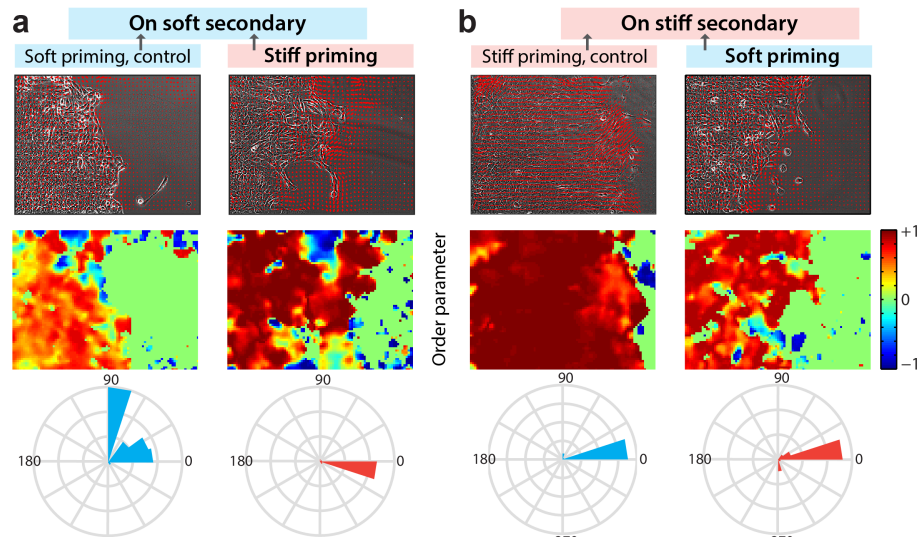


Figure S4: Alignment of single cell movement within the monolayer depends on primary ECM stiffness. Heatmap of order parameter (top row), vector field describing the direction of velocity vectors (middle row), and rose plot (bottom row) demonstrating the distribution of the angle between the instantaneous velocity vector and the x -axis, which were obtained by analyzing the trajectories of single cells for MCF-10A monolayer migrating on **(a)** soft and **(b)** stiff secondary ECM after being primed on soft or stiff primary ECMs.

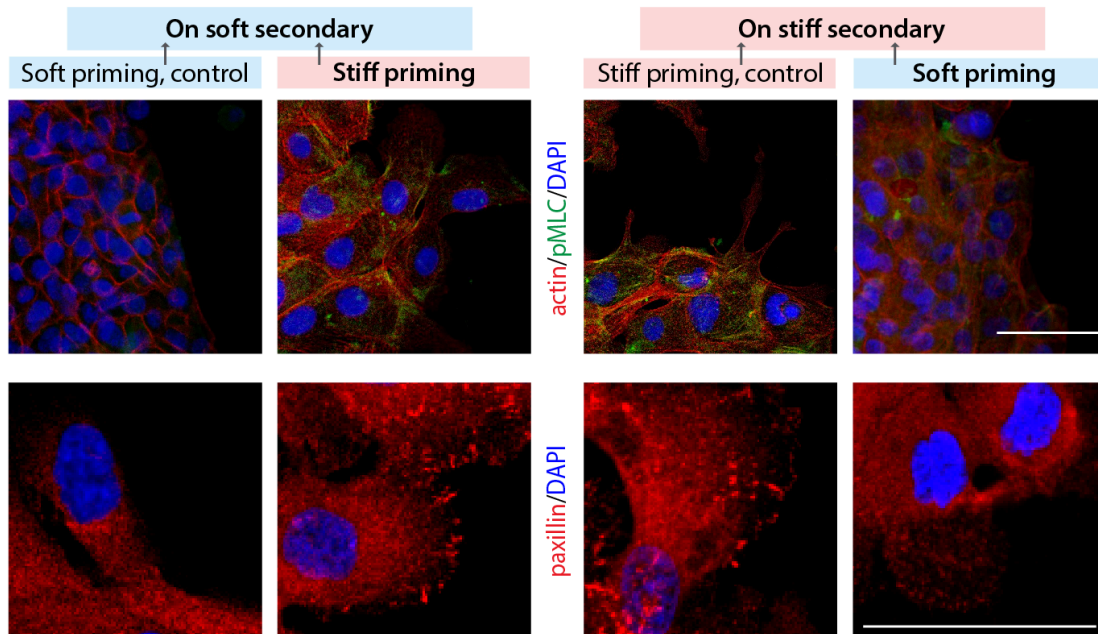


Figure S5: Immunofluorescent staining of pMLC (green), F-actin (phalloidin, red), and DAPI (blue) in top-panel and paxillin (red) and DAPI (blue) in bottom-panel for MCF10A cell monolayers on the secondary ECM after 2 days of migration (post-priming). Repeated from Figure 4 with higher resolution to better visualize actin fibers and punctate focal adhesions. Scale bar = 50 μ m.

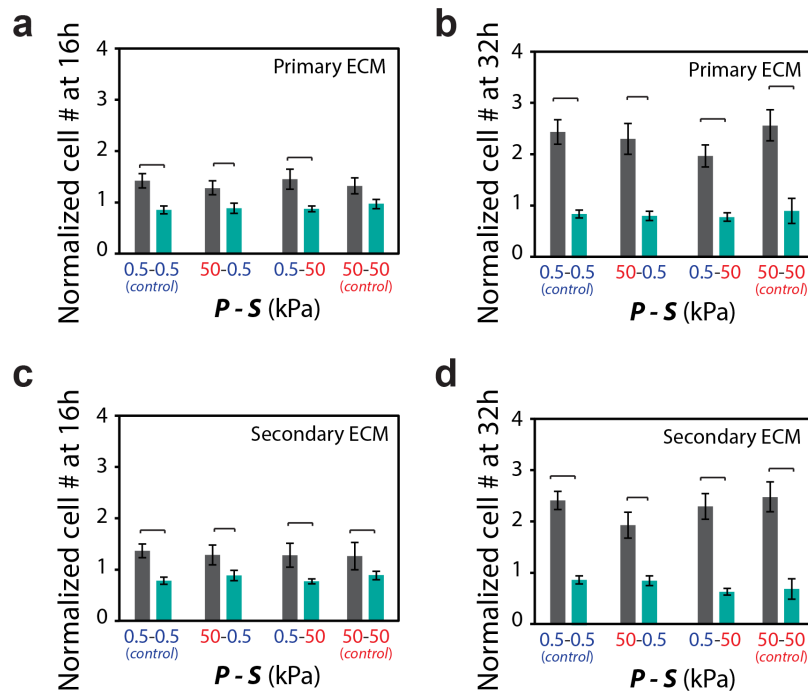


Figure S6: Number of cells after proliferation inhibition. (a-d) Normalized number of cells within a defined region of interest in primary and secondary ECMs at time $t=16h$ and $t=32h$ from $t=0$, the start of migration (post-priming), for thymidine-treated and untreated cells. Normalization performed relative to the number of cells in the RoI at $t=0$. Horizontal brackets denote statistical significance ($P < 0.05$). Error bars = SEM.

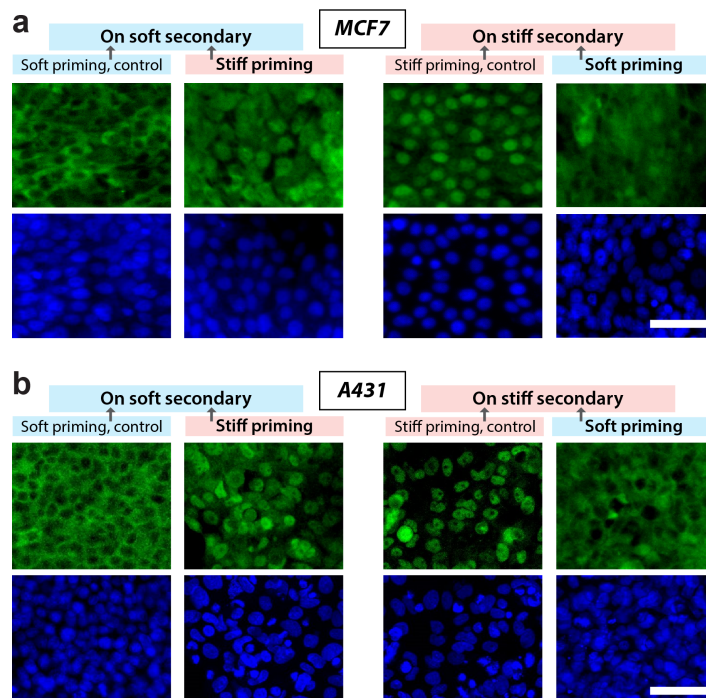


Figure S7: Representative images of YAP expression in MCF7 and A431 cells. Immunofluorescent staining of MCF-7 (a) and A431 (b) cells for YAP (green) and DAPI (blue), illustrates the subcellular localization of YAP for the monolayer migrating on soft and stiff secondary ECM, after priming on soft or stiff ECMs. Scale bar = 50 μm .

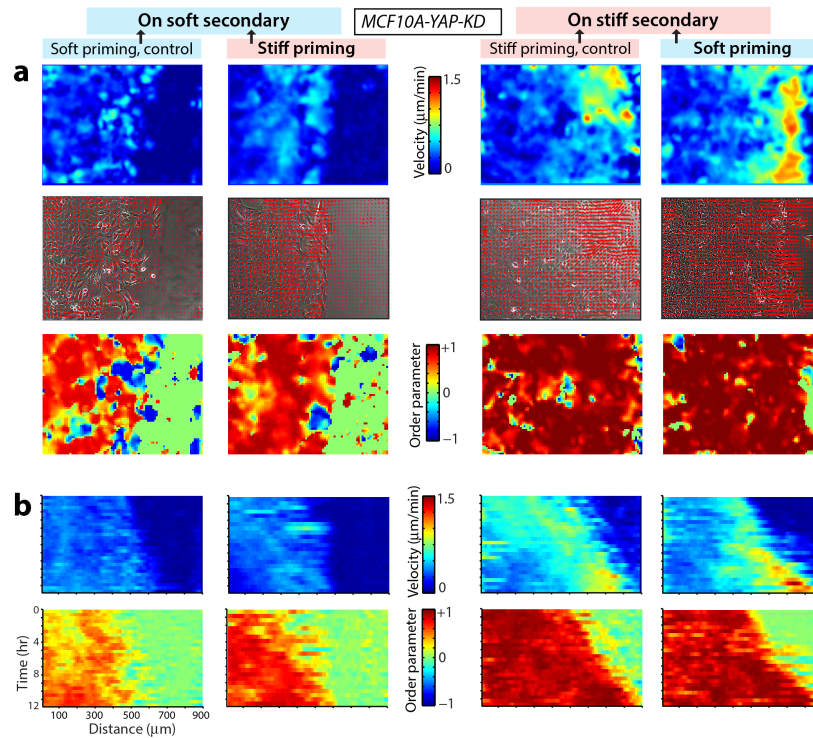


Figure S8: Monolayer dynamics in YAP-depleted MCF10A cells. (a) Heatmap showing the spatial distribution of velocity magnitude (top row), vector field describing the direction of velocity vectors (middle row), and order parameter (bottom row) at a given time instant for YAP-depleted MCF10A cell monolayer migrating on soft (left column) and stiff (right column) secondary ECMs, after priming on either stiff or soft primary ECMs. **(b)** Position-time kymographs of velocity magnitude and order parameter obtained from PIV analysis for corresponding ECM conditions described above to demonstrate the time evolution of monolayer motion. Kymographs were computed by averaging the velocity magnitude and order parameter of individual velocity vectors in the x direction over the y coordinate for every time point.

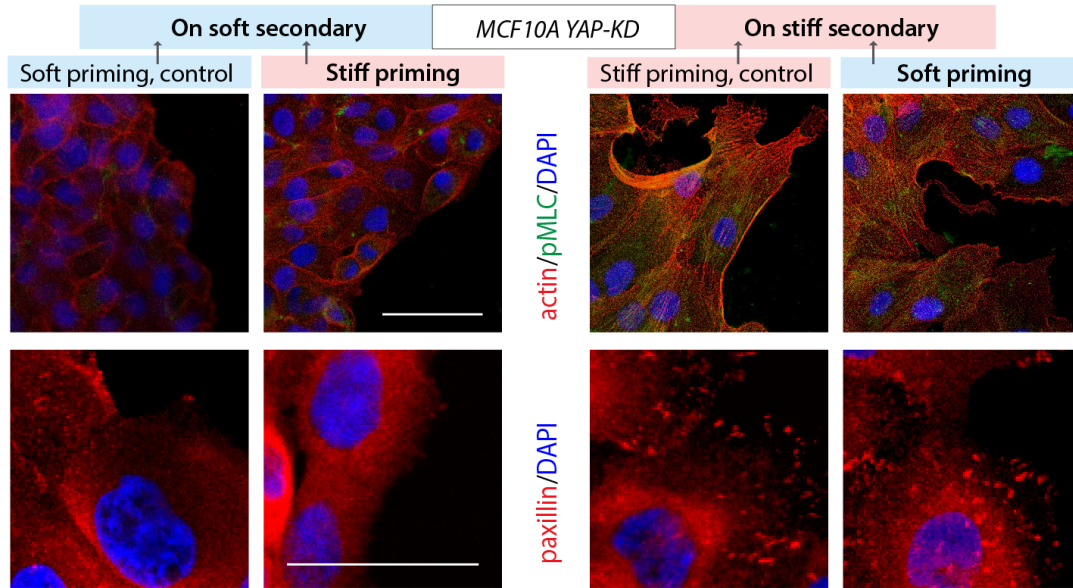


Figure S9: Immunofluorescent staining of pMLC (green), F-actin (phalloidin, red), and DAPI (blue) in top-panel and paxillin (red) and DAPI (blue) in bottom-panel for YAP-depleted MCF10A cell monolayers on the secondary ECM after 2 days of migration (post-priming). Repeated from Figure 7 with higher resolution to better visualize actin fibers and punctate focal adhesions. Scale bar = 50 μ m.

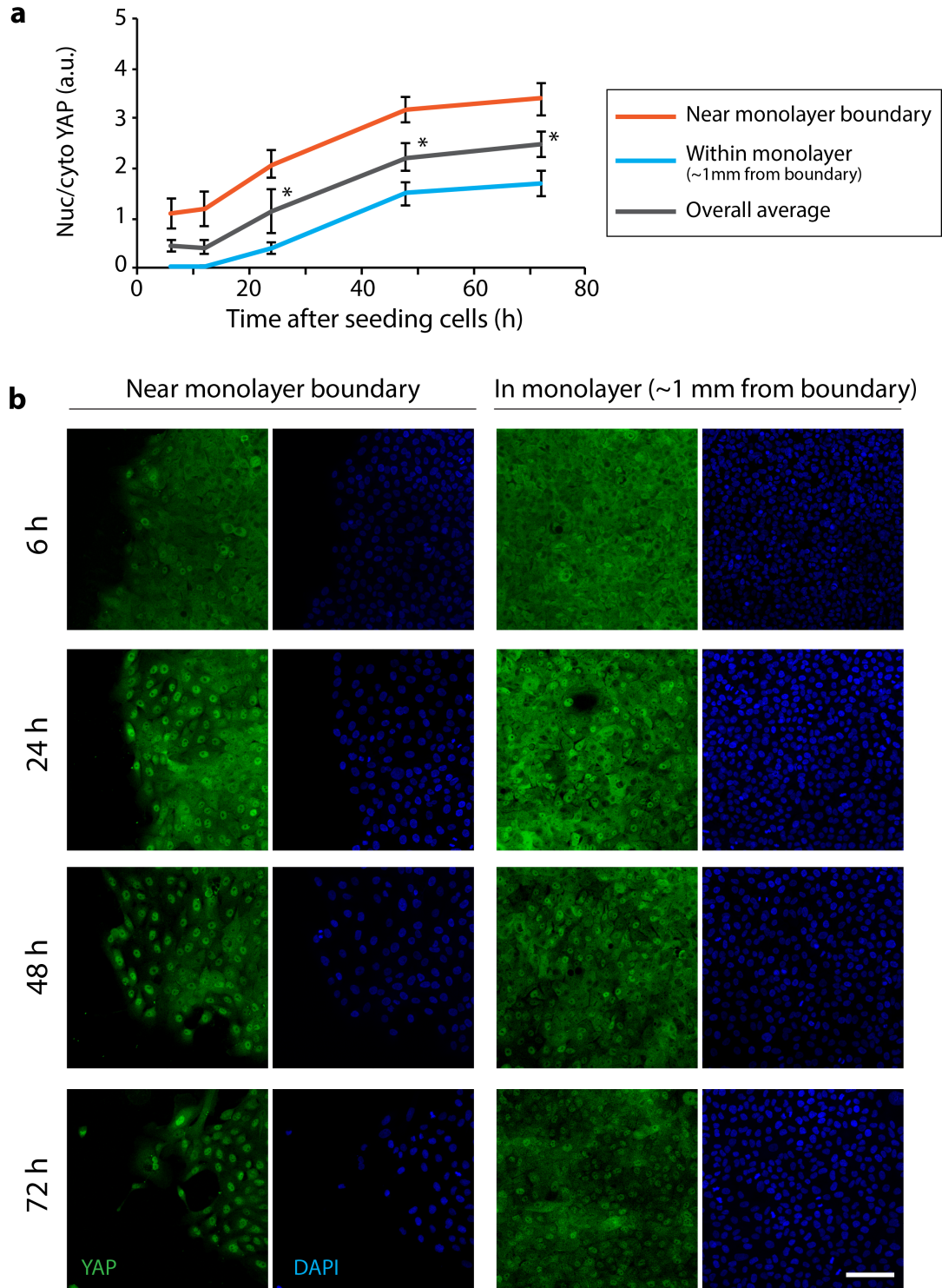


Figure S10: Time progression of YAP nuclear localization on stiff ECM. (a) Average nuclear-to-cytoplasmic ratio of the YAP fluorescent intensity for MCF10A cells cultured on stiff ECM (50kPa) located near the monolayer boundary (within 0.4mm; blue line), within the monolayer (~1mm away from the monolayer boundary; red line), and overall average (regardless

of location relative to the monolayer boundary; gray line) as a function of time after cell seeding. Mean values were obtained by analyzing >40 cells from >4 different fields of views from >2 experiments. * $p < 0.05$ with respect to the 6h data point. Error bars=SEM. **(b)** Immunofluorescent staining of MCF10A cells for YAP (green) and DAPI (blue) illustrating the nuclear localization of YAP for the monolayer cultured on stiff ECM, fixed at 6, 24, 48 and 72 h after seeding. Scale bar = 100 μm .